
Measurement of Cutting Torque by Speed Increasing Spindle

Masashi YAMANAKA¹, Shinji MIYAMURA², Katsumi INOUE¹
¹Tohoku University, ²SHOWA CORPORATION

Keywords: Cutting torque, Measurement, Speed increaser, End milling, Planetary gears

Abstract

A method of measuring cutting torque during milling using a small end mill, using a speed-increasing spindle with planetary gears is proposed. Its viability was confirmed by experiments using three types of end mill and the workpiece of NAK55. By attaching a few parts to a commercially available speed-increasing spindle, torque can be measured at a low cost. Using the torque measurement method proposed, it was experimentally demonstrated that the phenomenon that the higher the cutting speed, the smaller the cutting torque.

1. Introduction

The measurement of cutting torque during end milling is effective for the optimization of cutting conditions, the prediction of tool life and the prevention of tool failure [1]-[4]. A cutting force can be detected by attaching a dynamometer to a spindle in the machining center or a workpiece [5]. However, some problems remain; for example, the limitations of the milling range and the shape of the workpiece, and the high cost of equipment. Moreover, the power required for cutting can also be calculated by measuring the power consumption of the spindle motor [6][7]. However, it is difficult to measure a small load applied by a small-diameter tool when using a spindle with a large-capacity motor.

On the other hand, to obtain a good surface by milling using a small end mill, it is effective to increase cutting speed. Accordingly, a speed-increasing spindle may be used. Planetary gears are generally used for increasing speed [8] and planetary rollers with a traction drive are also commercially available [9]. In this study, we propose a method of measuring cutting torque during milling using a small end mill, using a speed-increasing spindle with planetary gears. By attaching a few parts to a commercially available speed-increasing spindle, torque can be measured at a low cost. Here, the principle of measurement and the evaluation of results obtained from the end milling experiments in the torque measurement method proposed are described.

2. Principle of Measurement

Planetary gears consist of three elements; namely, a sun gear, a ring gear and a carrier. In most cases, one is fixed and the other two are used as an input and an output. Depending on the transmission torque, a counter torque reacts in the fixed part. Therefore, the transmission torque can be calculated by measuring the magnitude of counter torque. In the case of the speed-increasing spindle with the planetary gears, the carrier and sun gear are used as an input and an output, respectively, and the ring gear is fixed. The end mill is fixed at the sun gear. We devised a mechanism, in which the arm is fixed at the ring gear and a load cell is set between the arm and a stopper, as shown in Fig. 1. The cutting torque applied on the sun gear during end milling can be calculated in the following procedure. The rotary counter force measured at the load cell is multiplied by the distance between the load cell and the center of the rotation, and then, the obtained value is divided by the transmission gear ratio between the ring gear and sun gear.

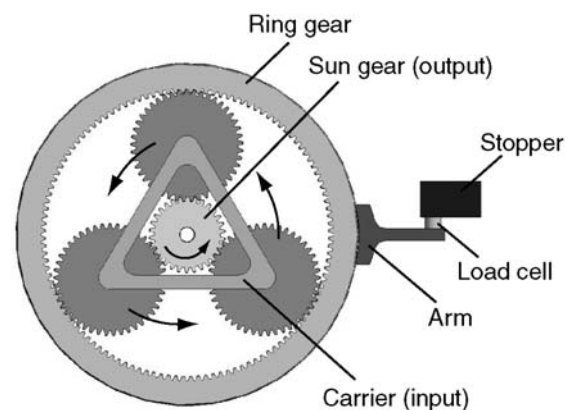


Fig. 1. Principle of torque measurement

3. Experimental Setup and Calculation Method of Cutting Torque

To verify that the cutting torque can be measured in the method proposed, a commercially available speed-increasing spindle with planetary gears was modified as shown in Fig. 2. A load cell was set between the arm and stopper, where a preload was applied using a bolt. Therefore, the force to be detected at the load cell is considered to be the sum of preload, force during idling and cutting force. The load cell output was input to a personal computer via an amplifier after A/D translation.

First, a static calibration was carried out in the following procedure. An L-shaped bar was fixed on the chuck, which is for grasping the end mill to be fixed. The bar was pulled with a spring scale in the rotational direction to give a torque. At that time, the load cell output was recorded. As shown in Fig. 3, the output force obtained was proportional to the tensile force, which is in agreement with the theory as mentioned above. Here, the speed increase ratio of the speed-increasing spindle used was 5.

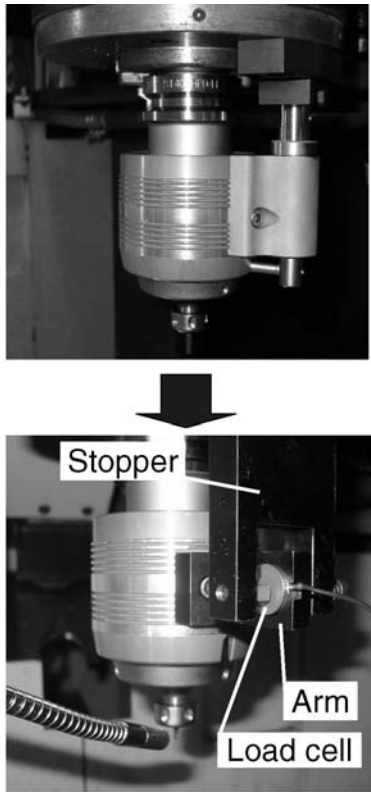


Fig. 2. Photograph of modified speed-increasing spindle with measurement devices

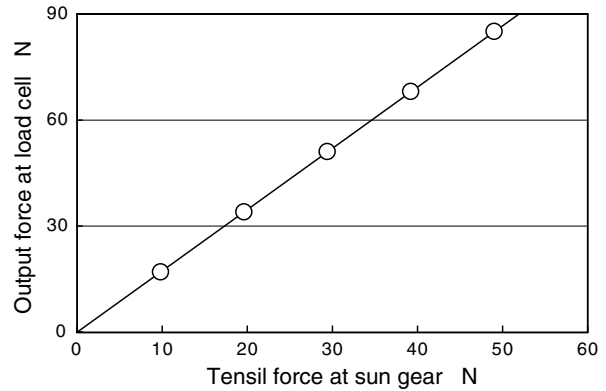
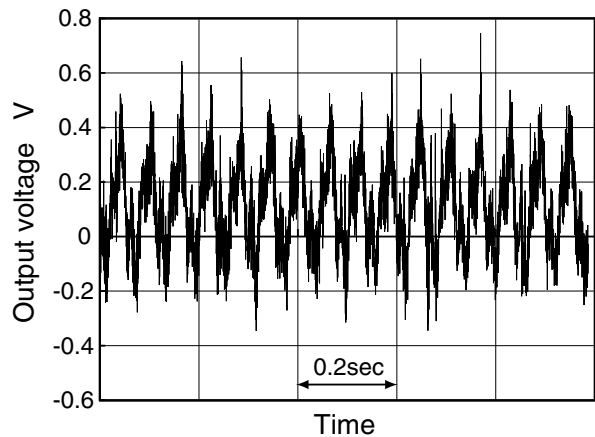


Fig. 3. Result of static calibration

Next, the output time response at the load cell during idling is shown in Fig. 4. The spectrum is also shown to have the characteristics of frequency response. The vertical axis indicates the half amplitude of the time response for the frequency. A strong peak appears at 16.7 Hz in Fig. 4. This is considered to be due to a torque irregularity occurring at the spindle motor because this frequency agrees with that of input rotary speed. Figure 5 shows the output time response at the load cell and its spectrum in the case of the end milling using the $\phi 2$ 2-flute end mill. The amplitude of the time response had few changes compared with that in Fig. 4. In the spectrum, a strong peak was observed at 167 Hz. Because the speed increase ratio of the speed-increasing spindle is 5 and the end mill has two flutes, if the carrier (input) rotates by one turn, the sun gear (output) rotates five times, resulting in a tenfold cutting rate. Accordingly, the peak caused by the milling was considered to appear at 167 Hz, which is the frequency tenfold that of the input waveform. This difference between the frequency component at milling and that at idling is considered to be the increase in frequency due to milling. When this value is converted to power, multiplied by the distance between the load cell and center of the rotation, and then, divided by the transmission gear ratio between the ring gear and the sun gear, which is 4, the cutting torque is obtained. However, real-time measurement has not been realized yet.



(a) Time response

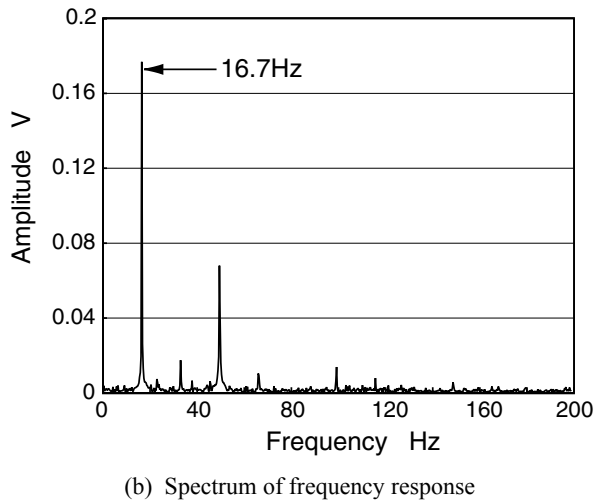


Fig. 4. Output of loadcell at idling

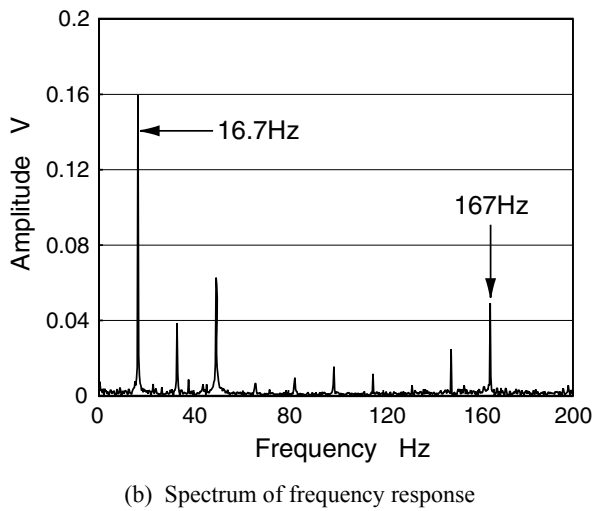
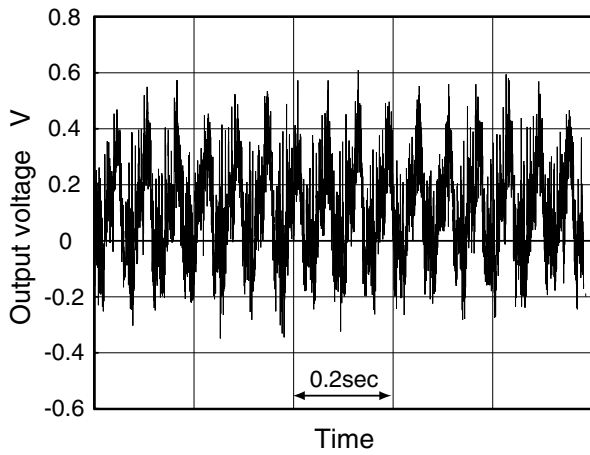


Fig. 5. Output of loadcell during end milling

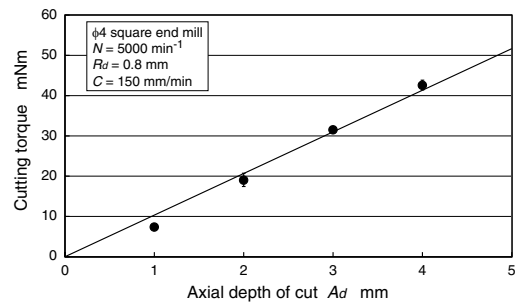
4. Results of Cutting Experiments

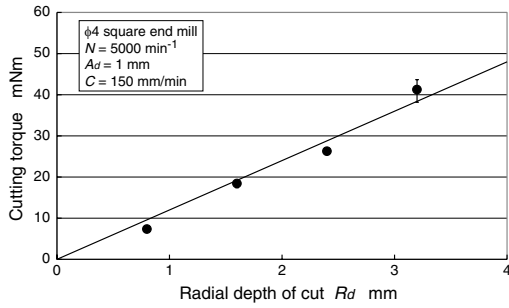
An end milling was carried out under various cutting conditions using three types of carbide end mill shown in Table 1 and cutting torque was measured in the method explained in §3. The material of the workpiece used was NAK55. All cutting conditions are shown in Table 1.

First, the end milling was carried out at a tool rotary speed N of 5000 min^{-1} with a variety of axial depths of cut, A_d , using a $\phi 4$ square end mill. The results of torque measurement during the end milling are shown in Fig. 6. The cutting torque was measured five times under each A_d condition and the mean value and dispersion of five torques measured are shown. The measured cutting torque increased with A_d . The results of the torque measurement obtained by varying the radial depth of cut, R_d , and the feed speed, C , are also shown in Fig. 6. Similarly to A_d , the values of cutting torque increased with R_d and C .

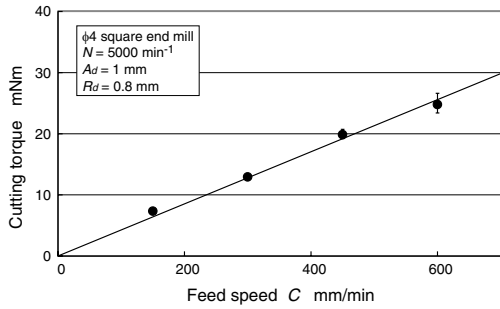
Table 1. Milling conditions

End mill	$\phi 4$ square	$\phi 2$ square	$\phi 2$ ball
Tool rotary speed [min-1]	5000, 20000	5000	
Cutting speed [m/min]	63, 251	31	
Axial depth of cut A_d [mm]	1 - 4	0.5 - 2	0.25
Radial depth of cut R_d [mm]	0.8 - 3.2	0.1 - 0.4	0.3
Feed speed C [mm/min]	150 - 1800	150 - 600	
Workpiece	NAK55		
Coolant	Dry		
Type of milling	Up cut		



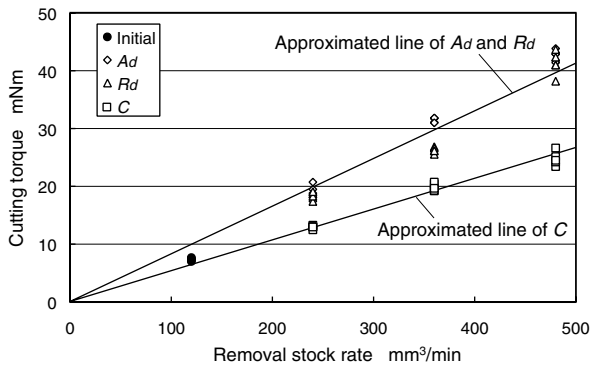


(b) Changing radial depth of cut

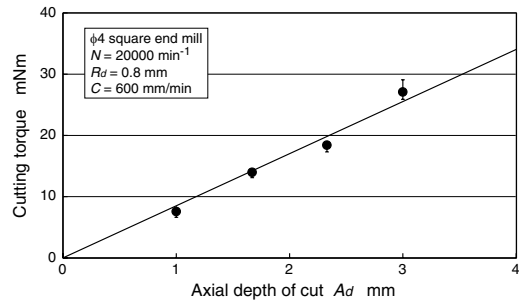


(c) Changing feed speed

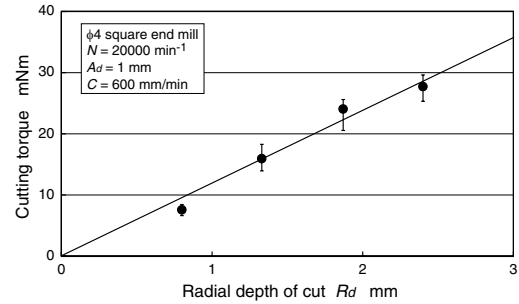
Fig. 6. Relation between cutting torque and milling condition



(a) Changing axial depth of cut



(b) Changing radial depth of cut



(c) Changing feed speed

torque owing to the increase in C is smaller than those owing to the increases in A_d and R_d . From these results, it was confirmed that torque could be measured despite different tool rotary speeds. Figure 10 shows a summary of the results shown in Figs. 7 and 9. When end milling at the same removal stock rate is carried out, the cutting torque in high-speed cutting, in which the tool rotary speed is high, is small. As generally known, this is because the volume of removal stock per revolution decreases when tool rotary speed is increased. Although calibration on the basis of the comparison using the dynamometer was not carried out, such a quantitative comparison is possible, showing the effectiveness of this measurement method.

Fig. 7. Relation between cutting torque and removal stock rate using $\phi 4$ endmill ($N=5000$)

Figure 7 shows the relationship between the removal stock rate and the cutting torque, which was obtained from the results shown in Fig. 6. The result of the measurement at $A_d = 1$ mm, $R_d = 8$ mm and $C = 150$ mm/min is also shown as an “initial” condition. The increased rate of cutting torque owing to the increase in A_d is almost the same as that owing to the increase in R_d . Compared with them, however, that owing to the increase in C is small. This result is in agreement with that in a previous report in which cutting resistance increases with an increase in C less than that in A_d or R_d . Similarly to the experiments shown in Fig. 6, experiments at $N=2000$ min⁻¹ were carried out, as shown in Fig. 8. The results had tendencies similar to those in the case of $N=5000$ min⁻¹. Namely, the measured cutting torque increased with A_d , R_d and C , and the increased rate of cutting

Fig. 8. Relation between cutting torque and milling condition

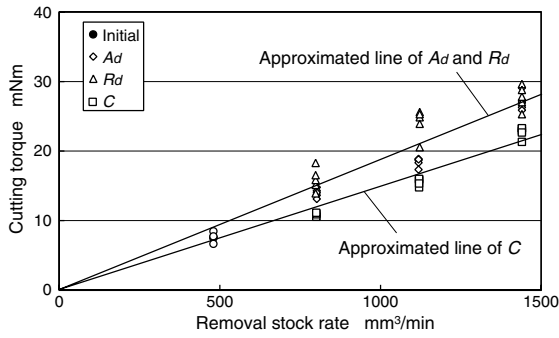


Fig. 9. Relation between cutting torque and removal stock rate using φ4 endmill ($N=20000$)

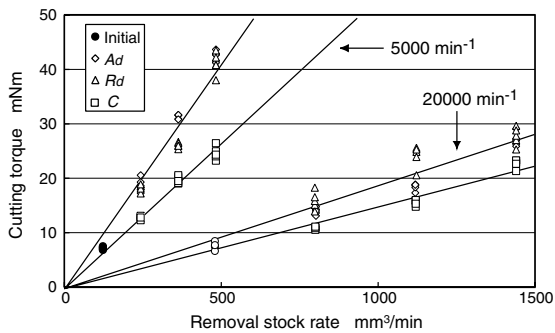


Fig. 10. Effect of high speed cutting

Next, the relationship between removal stock rate and cutting torque in the case of using the φ2 square end mill at $N=5000 \text{ min}^{-1}$ is shown in Fig. 11. Compared with the case of the φ4 square end mill, even though a little large dispersion was observed, a result similar to that in Fig. 7 was obtained. That is, the measured cutting torque increased with A_d , R_d and C , and the increased rate of cutting torque owing to the increase in C was smaller than those owing to the increases in A_d and R_d . From this result, it was confirmed that this measurement method is effective for the φ2 square end mill.

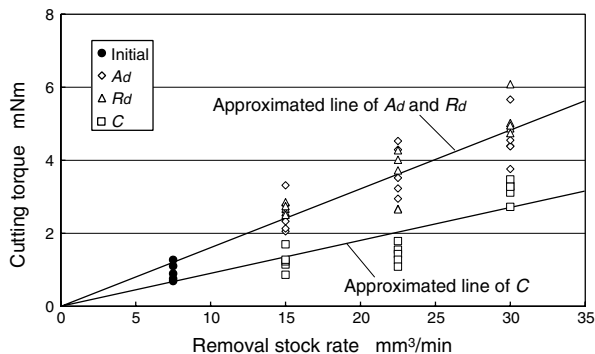


Fig. 11. Relation between cutting torque and removal stock rate using φ2 endmill ($N=5000$)

Figure 12 shows an example of the measurement of the cutting torque in the case of using a φ2 ball end mill at $N=5000 \text{ min}^{-1}$. Because the magnitudes of A_d and R_d are not proportional to the volume of removal stock in the case of end milling using the ball end mill, only C was varied. When C was increased, the measured cutting torque increased but the rate of increase in cutting torque decreased gradually. In that way, the characteristics of cutting torque during end milling in the cases of end mills with different shapes can be observed in this method.

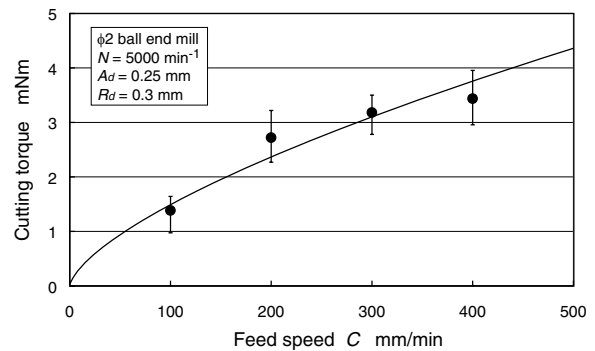


Fig. 12. Relation between cutting torque and feed speed using φ2 ball end mill

5. Conclusions

1. A method of measuring the cutting torque using a speed-increasing spindle was proposed and its viability was confirmed by experiments.
2. Using the torque measurement method proposed, it was experimentally demonstrated that the phenomenon that the higher the cutting speed, the smaller the cutting torque.

6. References

- [1] Tansel IN, Arkan TT, Bao WY, Mahedrakar N, Shisler B, Smith D, McCool M, (2000) Tool wear estimation in micro-machining. Part I: tool usage-cutting force relationship. *Int. J. Machine Tools & Manufacture* 40: 599-608
- [2] Masuda M, Nogami T, Mizobuchi A, Nagashima T, (2000) The behavior of tool life and cutting temperature on high speed milling of hardened alloy tool steels (in Japanese). *J. Japan Society for Precision Engineering* 66: 1745-1749
- [3] Miyaguchi T, Takeoka E, Masuda M, Iwabe H, (2001) Dynamic cutting force in high-speed milling using small ball end mill (in Japanese). *J. Japan Society for Precision Engineering* 67: 450-455

M. Yamanaka, S. Miyamura, K. Inoue

- [4] Oketani T, Mase Y, Nishigaki Y, Sase N, Fujii H, (1996) Development of a force sensing drill holder for fine drilling. J. Materials Processing Technology 56: 563-570
- [5] Kistler corporation, <http://www.kistler.com/>
- [6] KIM HY, Ahn JH, Kim SH, Takata S, (2002) Real-time drill wear estimation based on spindle motor power. J. Materials Processing Technology 124: 267-273
- [7] Stein JL, Wang CH, (1990) Analysis of power monitoring AC induction drive systems. ASME J. Dyn. Syst. Meas. Contr. 112:239-248
- [8] NT TOOL CORPORATION,
<http://www.nttool.com/english/index.html>
- [9] SHOWA TOOL CO., LTD,
<http://www.showatool.com/en/traction/index.html>